

Some experiences with BEPCII SRF system operation

Tong-ming Huang(黄彤明)^{1,2;1)} Hai-ying Lin(林海英)^{1,2} Yi Sun(孙毅)^{1,2}
 Jian-ping Dai(戴建坪)^{1,2} Guang-wei Wang(王光伟)^{1,2} Wei-min Pan(潘卫民)^{1,2}
 Zhong-quan Li(李中泉)^{1,2} Qiang Ma(马强)^{1,2} Qun-yao Wang(王群要)^{1,2}
 Guang-yuan Zhao(赵光远)^{1,2} Zheng-hui Mi(米正辉)^{1,2} Peng Sha(沙鹏)^{1,2}

¹ Institute of High Energy Physics, Chinese Academy of Sciences, Beijing 100049, China

² Key Laboratory of Particle Acceleration Physics and Technology, IHEP, Chinese Academy of Sciences, Beijing 100049, China

Abstract: The Superconducting Radio Frequency (SRF) system of the upgrade project of the Beijing Electron Positron Collider (BEPCII) has been in operation for almost 8 years. During operation, many problems have been encountered, such as excessive heating of the power couplers, frequent beam trips during high intensity colliding, false arc interlock trigger and so on. Among them, some has been solved successfully, some have been alleviated. This paper will describe some experiences with BEPCII SRF system operation, including the symptoms, causes and solutions of problems.

Keywords: superconducting radio frequency, superconducting cavity, power coupler, accelerator

PACS: 29.20.db **DOI:** 10.1088/1674-1137/40/6/067001

1 Introduction

The upgrade project of the Beijing Electron Positron Collider (BEPCII) has been in operation since the end of 2006. The machine was constructed for both high energy physics (HEP) and synchrotron radiation (SR) research. With the advantages of larger accelerating gradient, low RF power consumption and easier transmission-out of HOMs, a superconducting cavity (SCC) has been used in the BEPCII storage ring RF system [1]. The RF system consists of two independent sub-systems. Each one is composed of a 500 MHz SCC, a 250 kW klystron and a low level system. In collision mode, 1.5 MV accelerating voltage and 150 kW RF power can be provided to the positron ring (BPR) and electron ring (BER) separately.

Table 1. Main parameters of BEPCII SRF system [2].

parameters	collision mode	SR mode
frequency/MHz	499.8	499.8
cavity voltage/MV	2×1.5	2.0
energy loss per turn/keV	2×135	386
beam current/mA	2×910	250
beam power/kW	2×123	97
synchrotron phase /($^{\circ}$)	175	165
cavity number	2×1	1
klystron number	2×1	1
klystron power/kW	2×250	250
phase stability $\Delta\phi/(\text{^{\circ}})$	± 1.0	± 1.0
amplitude stability $\Delta V_a/V_a$ (%)	± 1.0	± 1.0

In SR mode, the beam circulates in the outer ring, and the system can provide 2.0 MV accelerating voltage and 100 kW RF power. The main parameters of the SRF system are listed in Table 1.

The SRF system has successfully worked at the design beam current of 910 mA, and the highest colliding luminosity ($8 \times 10^{32} \text{ cm}^{-2} \cdot \text{s}^{-1}$) was recorded in April 2014. However, many problems were encountered during operation. Overheating of the power coupler, frequent beam trips at high intensity collision, and false arc interlock trigger will be described in detail.

2 Power coupler overheating

Each SCC is fed through one power coupler. As shown in Table 1, each coupler has to deliver RF power up to 150 kW in continuous wave (CW) mode. The coupler is coaxial type, which consists of three parts: (1) a doorknob to realize the transition from waveguide to coaxial line; (2) an RF window to serve as an RF-transparent vacuum barrier; and (3) a 50 Ω coaxial line to transfer and feed RF power into the cavity [3]. During operation, overheating of the power coupler has always been a troublesome problem.

2.1 Doorknob overheating problem

During the annual operation from 2010 to 2011, the temperature of the doorknob located at the red point

Received 17 November 2014, Revised 26 November 2015

1) E-mail: huangtm@ihep.ac.cn

©2016 Chinese Physical Society and the Institute of High Energy Physics of the Chinese Academy of Sciences and the Institute of Modern Physics of the Chinese Academy of Sciences and IOP Publishing Ltd

of the ‘T_doorknob’ as shown in Fig. 1 increased above 46°C at the power level of 100 kW. A power leak was suspected to be the reason at the beginning, so the doorknob was reinstalled. However, the temperature was still too high. Then the air cooling efficiency was suspected and a careful thermal analysis was done. How air cooling impacts the doorknob temperature was analyzed by both simulation and measurement, as shown in Fig. 2 and Table 2. It can be concluded that the cooling air temperature should be around 20°C to keep the doorknob temperature below 40°C during 100 kW RF power operation. Finally, two large air conditioners were added to keep the cooling air temperature around 20°C. After that the doorknob overheating never happened again.

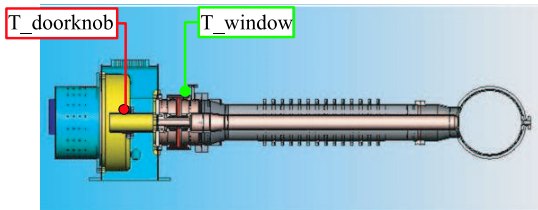


Fig. 1. (color online) 3D model of the power coupler: the areas noted with red and green point are overheating.

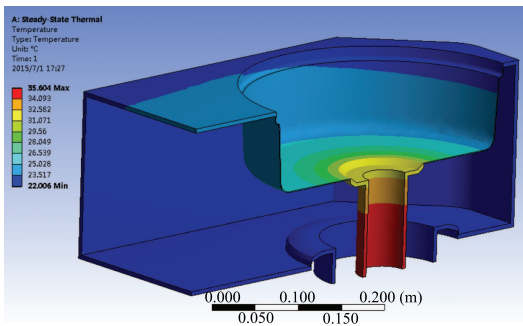


Fig. 2. (color online) The calculated doorknob temperature distribution with 100 kW RF power passing through and 20°C air cooling.

Table 2. The temperature of the doorknob with 100 kW RF power passing through.

cooling air temperature	calculated maximum “T_doorknob”	measured maximum “T_doorknob”
20°C	36°C	< 40°C
25°C	41°C	40–46°C
30°C	46°C	> 46°C

2.2 Window overheating problem

In Nov. 2013, the temperature of the window for the BPR power coupler was found to be excessively high after an arc interlock event, which became a big potential danger for the BPR SCC. In the worst case, the temperature of the window located at the green point of the

‘T_window’ as shown in Fig. 1 increased to 50°C in 5 minutes at the power level of 3 kW. Based on a series of experiments, the following characteristics were found. 1) The heating was very sensitive to the cavity detune angle. As shown in Fig. 3, at the power level of 40 kW, the temperature increased from 35°C to 54°C when the detune angle changed from 20° to –20°. 2) The heating is not uniform. The temperature of one side was 10°C higher than the opposite side at the same power level of 80 kW. Since the window structure is axis-symmetric, we can deduce that the abnormal heating source is located around one side of the planar ceramic. 3) After three times 150°C baking, the temperature rise reduced obviously, as can be seen from Fig. 4, which proved that the heating source is thermolabile. 4) The heating usually became more serious once some big outgassing happened. Figure 5 shows the typical vacuum pressure of both couplers, and we can see that the vacuum of the overheating window (BPR window: 7.5×10^{-8} Pa) is worse compared with the normal window (BER window: 5.5×10^{-8} Pa). Since discharging is usually caused by the interaction between the free electrons and the residual gases, it is more likely to occur in a worse vacuum condition. Table 3 lists the residual gasses of the overheating window during operation and 150°C baking, and it can be seen that the main outgasses are CO (or N₂), CO₂, H₂ and H₂O. So we speculate that the possible reasons for overheating are as follows. First, bad vacuum resulted in some serious discharging, then the discharging produced a large number of ions, which bombarded the copper surface, and then the sputtered copper reacted with the main residual gasses and formed some kind of copper compounds of CuC₂ or CuH. Finally, the copper compounds deposited on the ceramic surface, which resulted in the ceramic overheating. Fortunately, both CuC₂ and CuH are thermolabile. Their thermal decomposition temperatures (CuC₂:100°C, CuH:60°C) are below the baking temperature of 150°C, which can well explain why the problem can be alleviated by 150°C baking.

Though accurate verification of the above guess is difficult due to the infeasibility of disassembling the window, a similar simulation was done using ANSYS: an artificial lossy material was added on one side of the ceramic with 80 kW and 120 kW RF power passing through. The material was set as a thin slice (size: 10 mm×10 mm×1 mm). As can be seen from Fig. 6, the temperatures on the outer window are 44–46°C (at 80 kW) and 55–59°C (at 120 kW), which agree well with the measured values (43.8°C at 80 kW; 58.5°C at 120 kW); and the maximum temperature (59.8°C at 80 kW; 78°C at 120 kW) appears on the heating source side of the ceramic. The thermal stress was analyzed further, as shown in Fig. 7, and the maximum stress (60 MPa at 80 kW; 90 MPa at 120 kW) occurs on the

inner conductor of the ceramic. The ceramic tensile ultimate strength is about 240 MPa.

Base on the above analysis, two important conclusions can be drawn: 1) keeping a good vacuum is very important for power coupler safety; 2) if less than one quarter of the ceramic tensile ultimate strength is safe, the window temperature interlock value can be chosen as 45°C.

Up to now, the problem is just alleviated instead of eliminated. A close monitoring of the window temperature is done during actual beam operation.

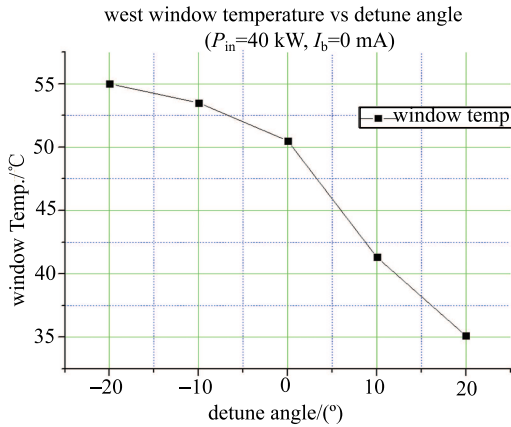


Fig. 3. (color online) Sensitivity of window temperature to the detune angle.

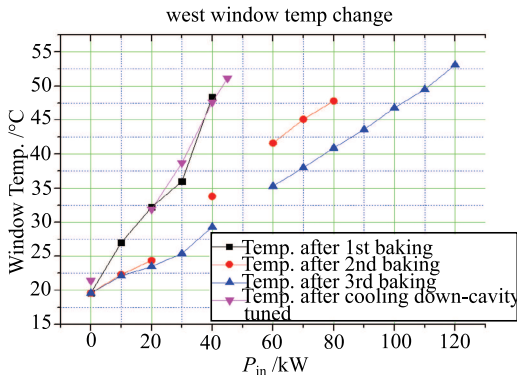


Fig. 4. (color online) 150°C baking is effective to alleviate the window overheating problem.

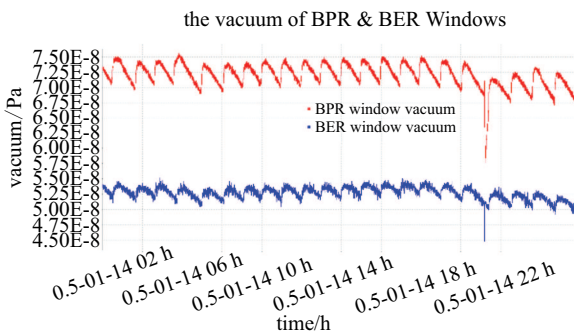
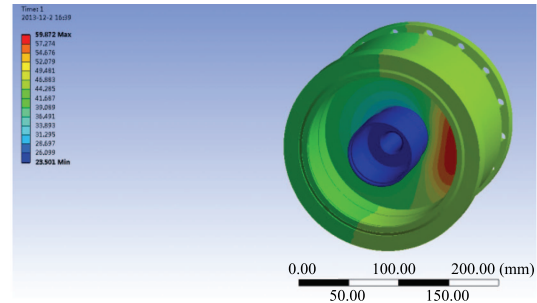


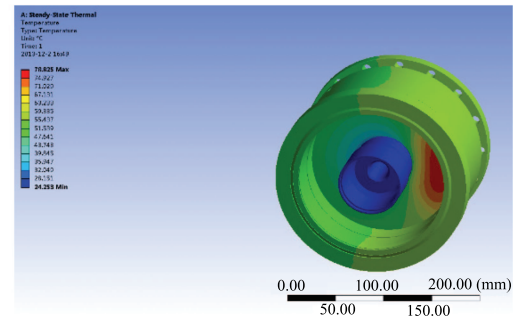
Fig. 5. (color online) BPR (top line) and BER (bottom line) window pressure.

Table 3. The residual gasses inside the couplers.

gasses	during baking	during operation
H ₂ (2)	6.1E-8 Torr	9.2E-9 Torr
HO(17)	1.0E-8 Torr	1.8E-9 Torr
H ₂ O(18)	2.3E-8 Torr	2.0E-9 Torr
CO or N ₂ (28)	3.7E-7 Torr	7.2E-8 Torr
Ar(40)	1.7E-8 Torr	5.5E-9 Torr
CO ₂ (44)	5.2E-8 Torr	4.8E-9 Torr



(a)



(b)

Fig. 6. (color online) The simulated window temperature with an artificial lossy material on one side of the ceramic: (a) 80 kW RF power passing through (max: 59°C, outer window: 44–46°C); (b) 120 kW RF power passing through (max: 78°C, outer window: 55–59°C).

3 Frequent beam trip during high intensity colliding

Frequent beam trips during high intensity collision, resulting in single beam or two-beam loss, has been a persistent problem and significantly limits the colliding efficiency. A multi-channel oscilloscope is used to record the signals of beam, cavity accelerating voltage, RF forward and reflection powers, vacuum pressure, RF phases and so on. With the trigger function, changes in the signals can be recorded within micro-seconds and shown graphically once a beam trip happens. Then, a preliminary analysis of the reason of trip can be done by distinguishing the time sequences and variation tendencies

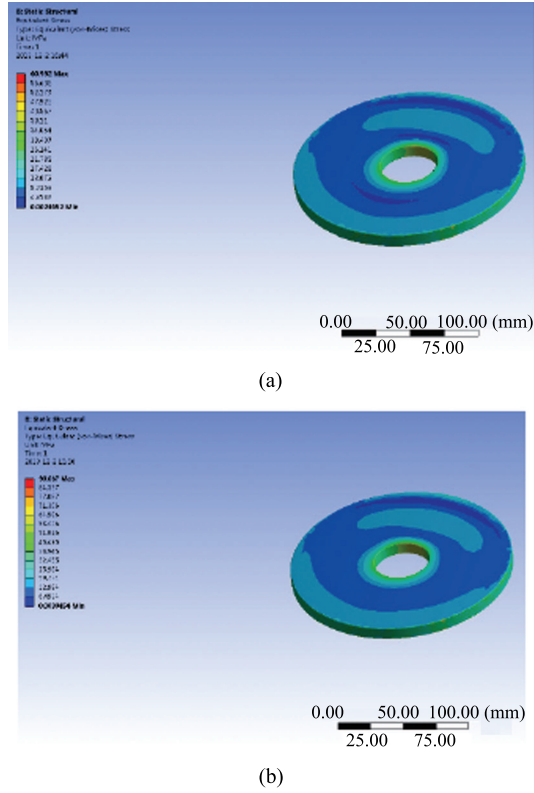


Fig. 7. (color online) The simulated ceramic equivalent stress with an artificial lossy material on one side of the ceramic: (a) 80 kW RF power passing through (max: 60 MPa); (b) 120 kW RF power passing through (max: 90 MPa).

of the signals. A bunch-by-bunch BPM system has also been built to analyze the reason for the trips [4]. The analysis results of the two methods are compared and agree well with each other.

An example is shown below. The BPR beam tripped suddenly after 50 minutes of colliding. The signal image recorded by the multi-channel oscilloscope is shown in Fig. 8. As can be seen, the positron (e^+ Beam) was lost in 10 ms, and the cavity accelerating voltage (Vc-W) and forward RF power (PF-W) were stable before the beam was lost. So we guess that beam instability resulted in this trip event. The analysis results from the bunch-by-bunch BPM system are shown in Fig. 9. The relative beam current in the process of the trip indicates that the beam started to oscillate 17000 turns before it went down to zero. In the time domain, the beam position shows that the beam oscillated seriously in the transverse direction; and in the frequency domain, the frequency spectrum amplitude at the half integer (0.5) is very high. Apparently the tune shifted to half integer and resulted in beam instability. The power supply system and magnet system are highly suspected.

Up to now, almost all the beam trips can be easily distinguished as beam instability, RF system trip, magnet and other system breakdowns such as power supply and cryogenics, which is very helpful to reduce the beam trip rate. Figure 10 shows the categorized pie chart of beam trips during 2013 to 2014 annual operation, from which can be seen that the RF system contributed 48%



Fig. 8. (color online) Beam trip image recorded by the multi-channel oscilloscope (201501111508). (Vc-W: BPR cavity voltage; Pr-W: BPR cavity reflection RF power; e^+ Beam: positron intensity; PF-W: BPR cavity forward RF power; vac-cpl: BPR cavity power coupler vacuum pressure; Pr_E: BER cavity reflection RF power; beam.pha: positron phase; Pf_E: BER cavity forward RF power; Vc-E: BER cavity voltage; vc pha_w: BPR cavity phase; e-beam: electron intensity).

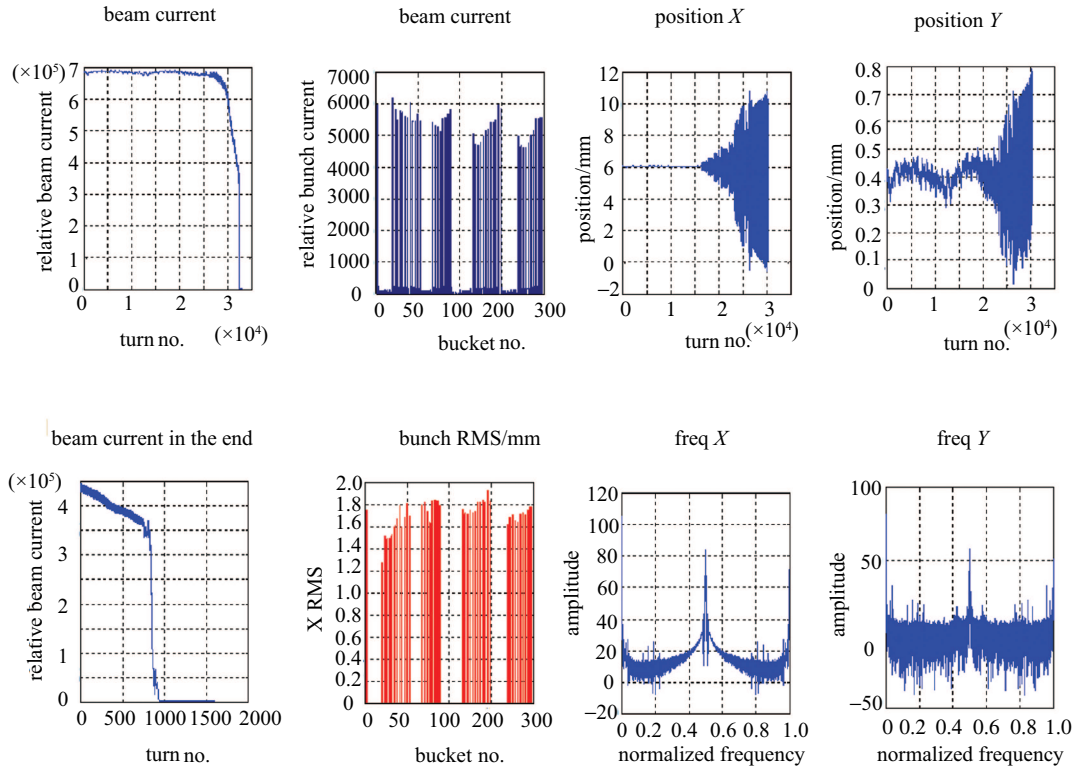


Fig. 9. (color online) Beam trip analysis results based on the bunch-by-bunch BPM system (201501111508).

to the beam trips. Among the RF system trips, the unclear BER cavity quench and the false BPR window arc were dominant (Fig. 11).

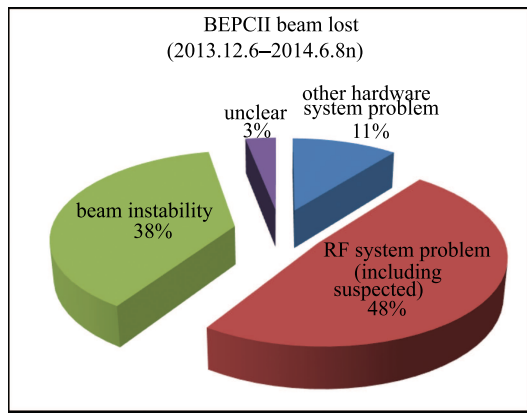


Fig. 10. (color online) Categorized pie chart of beam trips during 2013 to 2014 annual operation [5].

4 False arc interlock trigger

Two arc detectors are used to protect the power couplers, one for the BPR ring, and the other for the BER ring. Theoretically, the arc detector trigger is only connected to its corresponding ring. However, it sometimes triggered when the other ring trips. What is stranger

is that there is no accompanying outgassing for more than 90% of such cases. A series of steps have been taken to address this, such as improving the arc detector circuit to raise its anti-jamming capability and increasing the trigger threshold value. However, the problem still exists. An important point is that the arc detector is never triggered if the trip happened under no beam condition, so it is highly suspected that the fiber is disturbed by the beam loss induced X-rays, i.e. not because

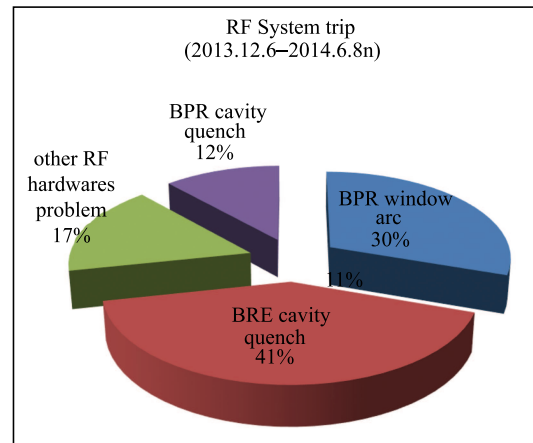


Fig. 11. (color online) Categorized pie chart of RF system trips during 2013 to 2014 annual operation.

of a real discharge inside the power coupler. A verification experiment was done: an additional fiber with the sensor packed by aluminum foil was arranged near the BPR cavity, i.e. the fiber sensor was not connected with the power coupler. The electron beam was then injected to 20 mA and kicked-off by the operator suddenly, and both the additional and the BPR coupler arc detector triggered simultaneously. This experiment proved the above speculation. A preliminary guess at the process is as follows: first, the lost beam induced X-rays; second, the X-ray penetrated into the fiber, interacted with the fiber and resulted in some electron transition; third, the electron transition produced some light which was captured by the arc detector. Based on the experiment, a lead shielding of the fiber was implemented. After that, the false arc trigger never happened in low beam intensity operation; however, it sometimes still occurs in high beam intensity operation. It is thought that the shielding could be improved by using thicker lead.

5 Summary

The SRF system for BEPCII has been in operation for almost 8 years and has successfully accelerated both electrons and positrons at the design beam current of 910 mA. During operation, many problems have been encountered. The doorknob of the power coupler was overheating, which was solved by reinforcing the air cooling; the window temperature of the BPR SCC power coupler was too high due to damage of the ceramic caused by discharging, which tells us that good vacuum pressure is very important for coupler safety; frequent beam trips during high intensity colliding has always been a persistent problem, until a trip diagnostic system was built, which is very helpful to reduce the trip rate; and the false arc interlock trigger was proved to be caused by beam loss- induced X-rays and partially solved by lead shielding of the fiber.

References

- 1 G. W. Wang et al, *BEPCII Accelerator Design and development* (Shanghai: SSMPF 2015), p. 245–250
- 2 G. W. Wang, P. Sha et al, *Chinese Physics C*, **32**(supplement): 169–171 (2008)
- 3 T. M. Huang, W. M. Pan et al, *Nuclear Instruments and Methods in Physics Research A*, 623: 895–902 (2010)
- 4 Q. Y. Deng et al, in *Proc. of IPAC2014* (Dresden, Germany, 2014), p. 2779–2782
- 5 T. M. Huang et al, *BEPCII SRF system 2013-2014 operation review*, edited by IHEP (Beijing: BEPC 18th Operation annual conference, 2014), p.75–85